Synthesis and Characterization of Hydrotris(pyrazolyl)borate Dihydrogen/Hydride Complexes of Rhodium and Iridium

Warren J. Oldham, Jr., Amber S. Hinkle, and D. M. Heinekey*

Contribution from the Department of Chemistry, University of Washington, Box 351700, Seattle, Washington 98195-1700

Received May 19, 1997[⊗]

Abstract: Protonation of $TpM(PR_3)H_2$ (M = Rh, Ir) complexes with $HBF_4 \cdot Et_2O$ or $[H(Et_2O)_2][B(Ar)_4]$ (Ar = 3,5-$(CF_3)_2C_6H_3$) affords cationic complexes which exhibit a single hydride resonance at all accessible temperatures in the ^1H NMR spectrum. Formulation as fluxional dihydrogen/hydride complexes is indicated by short $T_1(min)$ values of *ca.* 22 ms (Ir) and 7 ms (Rh). The relaxation times are consistent with H−H bond lengths of 0.88−1.11 Å in the iridium complexes and 0.73−0.92 Å in the rhodium complexes depending on the relative rate of the dihydrogen rotational motion. In the case of the iridium complexes, partial substitution of the hydride positions with deuterium or tritium results in large temperature-dependent isotope shifts and resolvable J_{H-D} or J_{H-T} coupling constants. Analysis of the chemical shift and coupling constant data as a function of temperature is consistent with a preference for the heavy hydrogen isotope to occupy the hydride rather than the dihydrogen site. This analysis also provides the limiting chemical shifts of the dihydrogen and hydride ligands as well as the $^1J_{H-D}$ coupling constant (*ca.* 25 Hz) in the bound dihydrogen ligand.
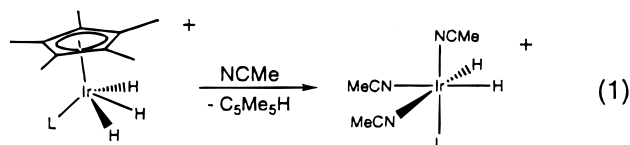
Since the first report of a stable molecular hydrogen complex by Kubas,[1] the possibility that a fluxional polyhydride complex might also contain a dihydrogen ligand has been actively investigated.[2] In general, transition metal polyhydride complexes are characterized by high coordination numbers (CN 7−9) and high formal oxidation states.[3] Because several structures of nearly equivalent energy are available to seven-, eight-, and nine-coordinate complexes, rapid permutation of the hydride positions is often observed by ^1H NMR spectroscopy. As a result, structural characterization in solution depends upon indirect methods, in which the observed NMR parameters are a population-weighted average of all the hydride environments. For example, Crabtree and co-workers have employed T_1 measurements to detect short H−H contacts in a range of polyhydride complexes, including $[Ir(PCy_3)_2H_6]^+$ and Fe-$(PEtPh_2)_3H_4$.[4] A quantitative treatment of relaxation in polyhydride complexes has been developed which allows useful structural information to be obtained from $T_1(min)$ data.[4−6]

We have previously reported the structure and properties of cationic iridium complexes of the form $[CpIr(L)H_3]BF_4$ (L = various PR_3), which have been shown to adopt iridium(V) trihydride structures in the solid state.[7,8] These complexes undergo a rapid hydride rearrangement which leads to a single hydride resonance in the ^1H NMR spectrum above *ca.* 220 K. However, at very low temperatures, spectra consistent with the solid state structure are obtained.

In this paper we investigate the effect of substituting the Cp ligand of $[CpIr(L)H_3]BF_4$ complexes with the hydrotris(1-pyrazolyl)borate (Tp)[9] ligand. The new Tp complexes, $[TpIr-(L)(H_2)H]BF_4$ (L = PMe_3, PPh_3), are formulated as dihydrogen/hydride complexes, although only a single hydride resonance is observed in the ^1H NMR spectrum at all accessible temperatures. We have also obtained spectroscopic evidence for the thermally labile rhodium complex $[TpRh(PPh_3)(H_2)H]^+$. Incorporation of deuterium or tritium in the hydride positions of the iridium complexes results in large temperature-dependent isotope shifts in the ^1H and ^3H NMR spectra, which are attributed to isotopic perturbation of equilibria. A similar isotope effect is not observed for the rhodium complex. We show that these isotope effects arise from nonstatistical occupation of different hydride sites and can be used to obtain structural information. Some aspects of the iridium chemistry have been previously communicated.[10]

Results

Synthesis. We have prepared complexes of the form $TpIr-(L)H_2$ (L = PMe_3, PPh_3) by two methods. The first approach was developed following a report by Pedersen and Tilset[11] that $[Cp^*Ir(PPh_3)H_3]BF_4$ reacts in acetonitrile to form $[(MeCN)_3Ir-(PPh_3)H_2]BF_4$ and free Cp^*H. We have found that the related PMe_3 complex $[Cp^*Ir(PMe_3)H_3]SO_3CF_3$ also reacts in acetonitrile to form $[(MeCN)_3Ir(PMe_3)H_2]SO_3CF_3$ (eq 1). The three

$$\text{(1)}$$

⊗ Abstract published in *Advance ACS Abstracts,* October 15, 1997.

(1) Kubas, G. J.; Ryan, R. R.; Swanson, B. I.; Vergamini, P. J.; Wasserman, H. J. *J. Am. Chem. Soc.* **1984,** *106,* 451−452.

(2) Heinekey, D. M.; Oldham, W. J., Jr. *Chem. Rev.* **1993,** *93,* 913−926.

(3) Hlatky, G. G.; Crabtree, R. H. *Coord. Chem. Rev.* **1985,** *65,* 1−48.

(4) Hamilton, D. G.; Crabtree, R. H. *J. Am. Chem. Soc.* **1988,** *110,* 4126−4133.

(5) Desrosiers, P. J.; Cai, L.; Lin, Z.; Richards, R.; Halpern, J. *J. Am. Chem. Soc.* **1991,** *113,* 4173−4184.

(6) Bautista, M. T.; Earl, K. A.; Maltby, P. A.; Morris, R. H.; Schweitzer, C. T.; Sella, A. *J. Am. Chem. Soc.* **1988,** *110,* 7031−7036.

(7) Heinekey, D. M.; Millar, J. M.; Koetzle, T. F.; Payne, N. G.; Zilm, K. W. *J. Am. Chem. Soc.* **1990,** *112,* 909−919.

(8) Heinekey, D. M.; Hinkle, A. S.; Close, J. D. *J. Am. Chem. Soc.* **1996,** *118,* 5353−5361.

(9) Substitution of the Tp ligand is represented by superscripts as suggested by Trofimenko. For example, methyl substituents in the 3,5-positions are indicated as Tp^{Me_2}. For a comprehensive review of this class of complexes see: Trofimenko, S. *Chem. Rev.* **1993,** *93,* 943−980.

(10) Heinekey, D. M.; Oldham, W. J., Jr. *J. Am. Chem. Soc.* **1994,** *116,* 3137−3138.

(11) Pedersen, A.; Tilset, M. *Organometallics* **1993,** *12,* 3064−3068.

Table 1.   Selected Spectroscopic Data for New Hydride Complexes

	^{1}H NMR (300 MHz, CD_2Cl_2)			IR (Nujol)	
complex	δ_{M-H} (ppm)	J_{P-H} (Hz)	T_1(min) (ms)	ν_{B-H} (cm^{-1})	ν_{Ir-H} (cm^{-1})
1	−21.30	25.0	542^a	2482	2142
2	−20.47	22.1	359^b	2481	2179, 2139
3	−22.11	26.7		2511	2138
4	−16.42	28.4^c	304^d	2475	2092, 2069
5	−10.40	11	21^e	2499	2199
6	−9.77	f	21^e	2502	2197
7	−11.0	f			
8	−7.95	f	7^g		

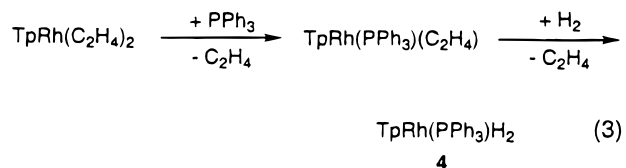^{a} 177 K. ^{b} 201 K. ^{c} J_{Rh-H} = 18.9 Hz. ^{d} 195 K. ^{e} 182 K. ^{f} Not resolved. ^{g} 180 K.

MeCN ligands of the new complexes are easily displaced by the pyrazolyl arms of the Tp ligand under mild conditions to form TpIr(L)H$_2$ (L = PMe$_3$ (**1**), PPh$_3$(**2**)). These reactions are conveniently carried out in one pot by generating the tris-(acetonitrile) intermediate *in situ* and then adding 1 equiv of NaTp in a second step. The procedure has also been used to prepare Tp^{Me_2}Ir(PMe$_3$)H$_2$ (**3**) upon addition of KTp^{Me_2} to a solution of [(MeCN)$_3$Ir(PMe$_3$)H$_2$]$^+$ in acetonitrile (eq 2).

$$[(MeCN)_3Ir(L)H_2]^+ \xrightarrow[\text{KTp}^{Me2}]{\text{NaTp or}} Tp^{R2}Ir(L)H_2 \qquad (2)$$
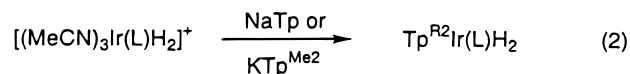
R = H, L = PMe$_3$ (**1**); R = H, L = PPh$_3$ (**2**);
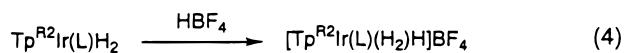R = Me, L = PMe$_3$ (**3**)

Complexes **1**−**3** are stable to air and water and can be purified by chromatography on alumina, eluting with toluene. Isolated yields are typically 55−70%. The dihydride complexes are colorless, thermally stable, and crystalline and are readily identified by their appropriate analytical and spectroscopic data, which are detailed in the Experimental Section. Selected spectroscopic data are reported in Table 1.

We have developed an alternative approach to these dihydride complexes using the reaction of phosphines with TpM(C$_2$H$_4$)$_2$ (M = Rh, Ir). The resulting TpM(PR$_3$)(C$_2$H$_4$) complexes react with hydrogen to afford the dihydride complexes in very good yield. For example, TpRh(PPh$_3$)H$_2$ (**4**) has been prepared using this method (eq 3). Characterization of the intermediate
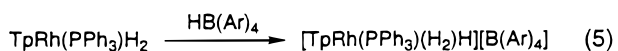
$$TpRh(C_2H_4)_2 \xrightarrow[\text{- C}_2\text{H}_4]{\text{+ PPh}_3} TpRh(PPh_3)(C_2H_4) \xrightarrow[\text{- C}_2\text{H}_4]{\text{+ H}_2}$$

$$TpRh(PPh_3)H_2 \qquad (3)$$
$$\textbf{4}$$

phosphine−ethylene complexes and the mechanism of their reaction with hydrogen has been separately reported.[12]

Addition of 1 equiv of HBF$_4$·Et$_2$O to CD$_2$Cl$_2$ solutions of **1**−**3** at ambient temperature or below affords new cationic complexes without elimination of H$_2$ (eq 4). The Tp^{Me_2} complex
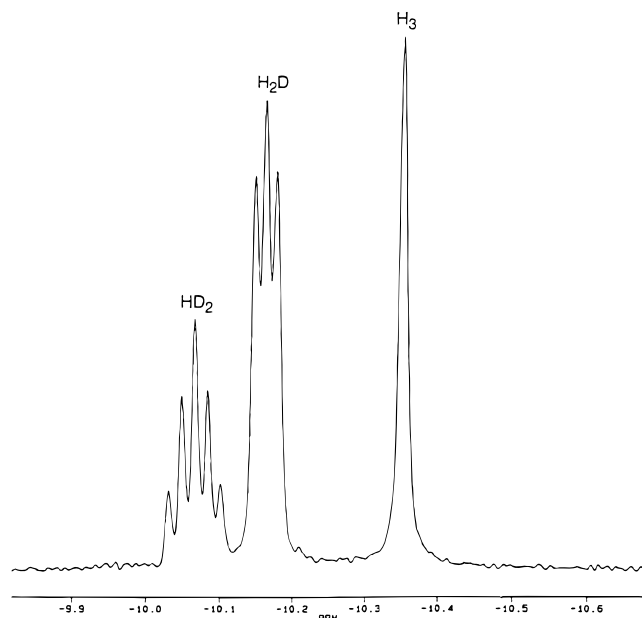
$$Tp^{R2}Ir(L)H_2 \xrightarrow{\text{HBF}_4} [Tp^{R2}Ir(L)(H_2)H]BF_4 \qquad (4)$$

1 - 3

R = H, L = PMe$_3$ (**5**) ; PPh$_3$ (**6**)

R = Me, L = PMe$_3$ (**7**)

$$TpRh(PPh_3)H_2 \xrightarrow{\text{HB(Ar)}_4} [TpRh(PPh_3)(H_2)H][B(Ar)_4] \qquad (5)$$

4   **8**

Figure 1. High-field region of the ^{1}H$\{^{31}$P$\}$ NMR spectrum (CD$_2$Cl$_2$, 500 MHz, 240 K) of a partially deuterated sample of [TpIr(PMe$_3$)-(H$_2$)]BF$_4$ (**5**).

decomposes at room temperature over the course of several hours; however, its lifetime in solution can be extended considerably if the protonation reaction is carried out with [H(Et$_2$O)$_2$][B(Ar)$_4$] (Ar = 3,5-(CF$_3$)$_2$C$_6$H$_3$). Similarly, **4** decomposes immediately at 210 K to a complex mixture of products upon addition of HBF$_4$·Et$_2$O. Reactions carried out with [H(Et$_2$O)$_2$][B(Ar)$_4$] yield [TpRh(PPh$_3$)(H$_2$)H][B(Ar)$_4$] (**8**), which is stable in solution to 250 K (eq 5). Complexes **5** and **6** were found to be thermally stable and can be isolated as colorless salts upon addition of HBF$_4$·Et$_2$O to Et$_2$O or Et$_2$O/CH$_2$Cl$_2$ solutions of the parent dihydride complexes.

Selected data for the new cationic hydride complexes are presented in Table 1. Complexes **5**−**8** exhibit a 2:1 pattern of Tp resonances in the ^{1}H and ^{13}C NMR spectra, which is characteristic of a structure with C_s symmetry. In all cases, this pattern is unchanged upon cooling to 180 K. An appropriate resonance for the respective hydride ligands is observed at high field near −10.4 ppm in the ^{1}H NMR spectra of **5**−**7**. A similar resonance at −7.95 ppm is observed for the rhodium complex **8**. Generally these resonances are broad with no distinguishing features. However, in the case of complex **5**, the hydride resonance is a doublet with P−H coupling of 11 Hz. A total of three hydride ligands (no structure implied) is confirmed by the observation of a quartet for the PMe$_3$ resonance in the ^{31}P-$\{$Me ^{1}H$\}$ NMR spectrum at −42.7 ppm (J_{P-H} = 10 Hz). For complex **5**, a sharp IR absorption at 2199 cm^{-1} is attributed to an Ir−H stretch and a band at 2499 cm^{-1} is assigned to the B−H stretch. Similar observations were made for **6**. The minimum of the longitudinal relaxation time (T_1) is found to be 21−22 ms for **5** and **6** but is 7 ms for **8**.

NMR Observations for Partially Deuterated Complexes. Deuteration of the hydride positions is observed over the course of several hours at room temperature upon exposure of solutions of **5**−**7** to an atmosphere of D$_2$. Well-resolved signals for H$_3$, H$_2$D, and HD$_2$ isotopomers are observed by ^{1}H NMR spectroscopy. Large temperature-dependent *downfield* isotope shifts are noted for the hydride resonances of the deuterated complexes. A representative spectrum of the hydride region for complex **5** acquired with ^{31}P decoupling at 240 K is shown in Figure 1.

(12) Oldham, W. J., Jr.; Heinekey, D. M. *Organometallics* **1997**, *16*, 467−474.

11030 *J. Am. Chem. Soc., Vol. 119, No. 45, 1997*

Oldham et al.
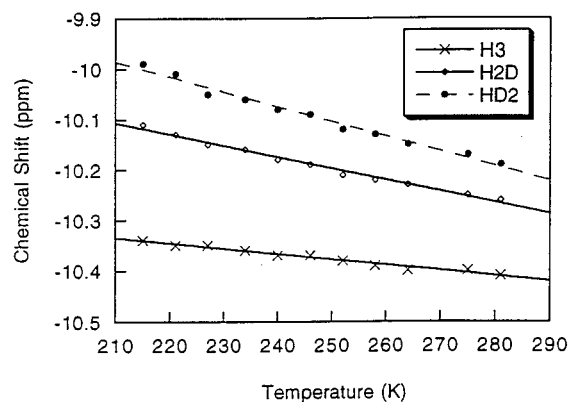
Figure 2. Plot of chemical shift of the hydride resonance in **5**, **5**-d_1, and **5**-d_2 as a function of observation temperature.
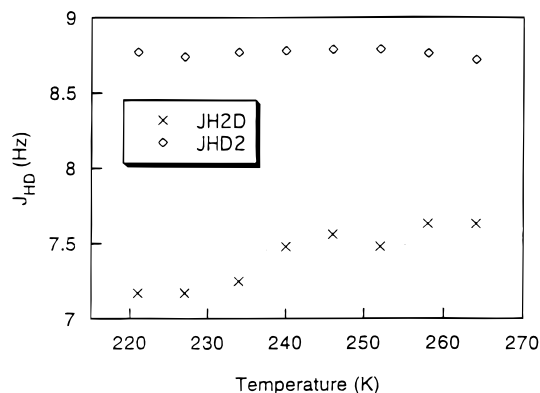
Figure 3. Plot of H−D coupling in **5**-d_1 and **5**-d_2 as a function of observation temperature.

The resonances of the Tp and phosphine ligands are unaffected by deuteration of the hydride positions and show no unusual temperature dependence. The isotope shifts for **5**, $\Delta_1 = \delta(H_2D) - \delta(H_3)$ and $\Delta_2 = \delta(HD_2) - \delta(H_2D)$, vary from +228 and +122 ppb at 215 K to +149 and +72 ppb at 280 K, respectively. Over a similar temperature range, the observed H−D coupling of the hydride resonance varies from *ca.* 6.9 to 7.6 Hz for **5**-d_1 and from *ca.* 8.8 to 8.7 Hz for **5**-d_2. These observations are represented graphically in Figures 2 and 3. Very similar temperature-dependent isotope shifts and H−D coupling constants are observed for **6** and **7**. The hydride resonances of the H$_2$D and HD$_2$ isotopomers of **6** are significantly broadened compared to those of **5** and **7**, so that the J_{H-D} coupling constant could not be accurately measured in this case. However, on the basis of the line width of the hydride peaks, the J_{H-D} coupling constants of **6** are similar to those measured for **5** and **7**. Data for these complexes acquired at 240 K are summarized in Table 2.

Complex **8** fails to exchange with D$_2$ under the low-temperature conditions at which it is stable. In this case, partial deuteration of the hydride positions was accomplished by reacting TpRh(PPh$_3$)D$_2$ with 1 equiv of [H(Et$_2$O)$_2$][B(Ar)$_4$] at low temperature. The hydride positions are estimated to contain *ca.* 55% deuterium by integration of the hydride resonance against the Tp resonances in the ^{1}H NMR spectrum (one scan). A broad featureless hydride resonance at the same chemical shift as that of the undeuterated complex is observed for the mixture of **8**, **8**-d_1, and **8**-d_2. The chemical shift of this resonance shows no significant temperature dependence.

A CDCl$_2$F solution composed principally of **5**-d_2 was investigated at low temperature by ^{1}H NMR spectroscopy. As the temperature was lowered, the hydride resonance of the HD$_2$ isotopomer continued to shift downfield; however, no evidence for decoalescence of this resonance was observed to 127 K. At

Table 2. Chemical Shifts of Hydride Resonances and J_{H-D} Coupling Constants for Partially Deuterated Isotopomers of Complexes **5**−**8**

complex	isotopomer	hydride shift (ppm)	J_{H-D} (Hz)
5[a]	H$_3$	−10.37	
	H$_2$D	−10.18	7.48
	HD$_2$	−10.08	8.78
6[a]	H$_3$	−9.80	
	H$_2$D	−9.61	*b*
	HD$_2$	−9.52	*b*
7[a]	H$_3$	−11.06	
	H$_2$D	−10.84	7.33
	HD$_2$	−10.75	8.90
8[c]	H$_3$	−7.96	*d*
	H$_3$, H$_2$D, HD$_2$	−7.94	*e*

[a] ^{1}H{^{31}H} NMR (500 MHz, 240 K). [b] Not resolved. [c] ^{1}H NMR (300 MHz, 213 K). [d] Broad; line width = 75 Hz. [e] Broad; line width = 63 Hz.
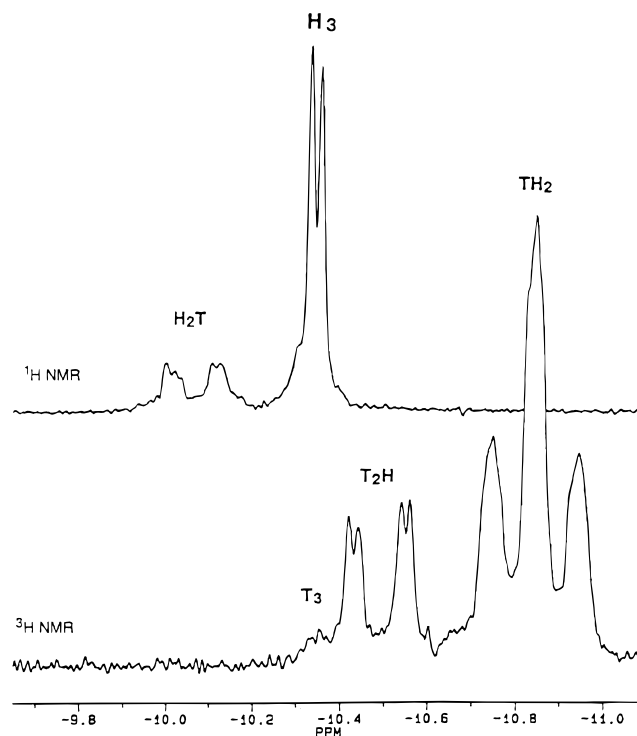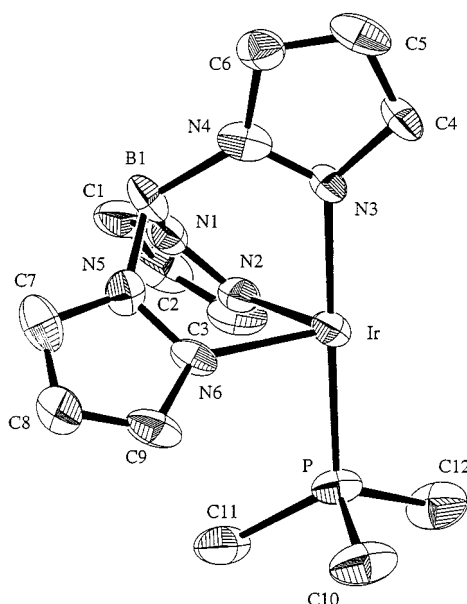

Figure 4. Top: ^{1}H NMR spectrum (CD$_2$Cl$_2$, 500 MHz) of a partially tritiated sample of **5**. Bottom: ^{3}H NMR spectrum (CD$_2$Cl$_2$, 533 MHz).

this temperature, the hydride resonance is observed at −9.64 ppm. Although the hydride resonance of the H$_3$ isotopomer cannot be observed at this temperature due to efficient dipolar relaxation, we estimate its chemical shift to be *ca.* −10.3 ppm. The isotope shift, $\delta(HD_2) - \delta(H_3)$, at this temperature is then *ca.* 660 ppb.

NMR Spectra of Partially Tritiated Complexes. Incorporation of tritium into the hydride positions of **5**−**7** was observed when CD$_2$Cl$_2$ solutions were exposed to T$_2$ gas (*ca.* 200 Torr) for several hours at room temperature. Distinct hydride resonances for the H$_3$ and H$_2$T isotopomers were observed in the ^{1}H NMR spectrum. The central peak of the HT$_2$ triplet was observed in the case of **6** and **7** but was not detected for **5** because the concentration of the HT$_2$ isotopomer was too small. The sample activity in each case is estimated to be less than 10 mCi. For **5**, the hydride resonance of the H$_2$T isotopomer is shifted *downfield* of the H$_3$ isotopomer by 280 ppb at 240 K (Figure 4). The H$_2$T resonance appears as a broad doublet of doublets due to coupling to phosphorus (J_{P-H} = 9.9 Hz) and tritium (J_{T-H} = 54.5 Hz). The hydride resonance of the H$_3$ isotopomer is a doublet (J_{P-H} = 11.6 Hz), due to coupling to phosphorus (see Figure 4).

Table 3. Hydride Chemical Shifts and J_{P-H}, J_{P-T}, and J_{H-T} Coupling Constants for Partially Tritiated Isotopomers of **5**−**7** observed by ^{1}H and ^{3}H NMR Spectroscopy at 240 K

complex		isotopomer	δ (ppm)	J_{P-H} or J_{P-T} (Hz)	J_{H-T} (Hz)
5	^{1}H NMR	H_3	−10.35	11.6	
		H_2T	−10.07	9.9	54.5
5	^{3}H NMR	T_3	−10.35	12.9	
		T_2H	−10.50	11.5	63.3
		TH_2	−10.75	a	53.2
6	^{1}H NMR	H_3	−9.70	9.1	
		H_2T	−9.44	a	52.6
		HT_2	−9.23	a	a
6	^{3}H NMR	T_3	−9.70	a	
		TH_2	−10.16	11.6	52.2
7	^{1}H NMR	H_3	−11.06	11.9	
		H_2T	−10.75	a	51.7
		HT_2	−10.52	a	a
7	^{3}H NMR	T_3	−11.06	a	
		T_2H	−11.22	a	65.7
		TH_2	−11.62	a	51.0

^{a} Not resolved.

Figure 5. ORTEP drawing (50% probability ellipsoids) for [TpIr-(PMe₃)(H₂)H]BF₄. Hydrogen atoms have been omitted for clarity.

In the ^{3}H NMR spectrum, distinct hydride resonances for the T_3, T_2H, and TH_2 isotopomers were observed. The T_2H and TH_2 isotopomers are shifted significantly *upfield* of the T_3 isotopomer. The isotope shifts at 240 K, $\Delta_3 = \delta(T_2H) - \delta(T_3)$ and $\Delta_4 = \delta(TH_2) - \delta(T_2H)$ are −150 and −250 ppb, respectively. The T_3 isotopomer was observed at the same chemical shift as the H_3 isotopomer in the ^{1}H NMR spectrum. The T_2H isotopomer appears as a doublet of doublets coupling to phosphorus ($J_{P-T} = 11.5$ Hz) and hydrogen ($J_{T-H} = 63.3$ Hz). The TH_2 isotopomer is a broad triplet with an observed T−H coupling constant of 53.2 Hz, which is identical within experimental error to the H−T coupling constant observed for the H_2T isotopomer in the ^{1}H NMR spectrum. The ^{1}H and ^{3}H NMR data for **5**−**7** are summarized in Table 3.

Structural Characterization. Crystals of **5**·CH₂Cl₂ suitable for X-ray diffraction were obtained by slow diffusion of Et₂O into a concentrated CH₂Cl₂ solution of **5**. An ORTEP drawing of the iridium cation and key structural features are given in Figure 5 and Table 4, respectively. The hydrogen atoms, BF₄⁻ anion, and the CH₂Cl₂ of crystallization have been omitted for clarity. The metal-bound dihydrogen ligand and the hydride ligand were not reliably located. No unusual intermolecular interaction between BF₄⁻ and the iridium metal center is

Table 4. Significant Bond Distances and Angles for **5**·CH₂Cl₂

Distances (Å)			
Ir−P	2.280(3)	Ir−N(2)	2.161(8)
Ir−N(3)	2.105(7)	Ir−N(6)	2.070(8)
P−C(10)	1.772(12)	P−C(11)	1.805(10)
P−C(12)	1.795(11)		
Angles (deg)			
P−Ir−N(2)	96.0(2)	P−Ir−N(3)	177.6(2)
N(2)−Ir−N(3)	86.3(3)	P−Ir−N(6)	94.(2)
N(2)−Ir−N(6)	84.3(3)	N(3)−Ir−N(6)	85.5(3)
Ir−P−C(10)	115.0(4)	Ir−P−C(11)	114.0(4)
Ir−P−C(12)	114.0(4)	B−Ir−P	128.6(2)

observed. The closest Ir−F contact is 3.541(15) Å. The closest contact between iridium and the CH₂Cl₂ of crystallization is 3.832(15) Å. The bond lengths and bond angles observed for **5**·CH₂Cl₂ are typical of Ir(III) Tp complexes.[13,14] The Ir−N bond distances to the equatorial pyrazolyl ligands are significantly different (2.161(8) vs 2.070(8) Å), which may relate to the hydride structure. Details of the structure solution and refinement are included in the Experimental Section.

Discussion

Synthesis. In contrast to the well-developed synthetic routes used to prepare Cp*Ir(PR₃)H₂ and CpIr(PR₃)H₂ complexes, similar approaches for the corresponding Tp complexes are unsuccessful. The immediate precursor to Cp*Ir(PR₃)H₂ is the corresponding dichloride complex. These are easily obtained upon reaction of [Cp*IrCl₂]₂ with a range of phosphine donor ligands.[15] Attempts by Powell and co-workers to prepare Tp^R₂-Ir(L)Cl₂ complexes from [Tp^R₂IrCl₂]₂ were reported to fail except in the case of L = AsPhMe₂.[16] The diiodide complexes CpIr(PR₃)I₂ employed in the Cp chemistry are prepared in a one-pot reaction from CpIr(C₂H₄)₂.[7] Both ethylene ligands are displaced upon addition of 1 equiv of I₂ to afford an iodide-bridged oligomer, [CpIrI₂]ₙ, to which 1 equiv of phosphine is added in a second step to yield CpIr(PR₃)I₂. We have found that TpIr(C₂H₄)₂ reacts with I₂ to yield [TpIr(C₂H₄)₂I]I, which reacts with PPh₃ to give [TpIr(PPh₃)(C₂H₄)I]I.[17] The ethylene ligand in this complex is not easily displaced.

We find that the TpIr(PR₃)H₂ complexes can be prepared from [(MeCN)₃Ir(PR₃)H₂]⁺, which is readily available by the reaction of acetonitrile with [Cp*Ir(PR₃)H₃]⁺ as reported by Tilset and Petersen. A more efficient approach involves reacting TpIr(C₂H₄)₂ sequentially with 1 equiv of a phosphine ligand and then adding H₂ in a second step to give TpIr(PR₃)H₂. This reaction is easily extended to include the related rhodium complexes. The details of this chemistry are reported separately.[12] A preparation of complex **3** by thermolysis of Tp^Me₂-IrH₄ with PMe₃ has been briefly reported, but no details of characterization were given.[18]

Characterization of the Cationic Hydride Complexes. The cationic species resulting from protonation of **1**−**4** give spectroscopic data consistent with new complexes containing a mirror plane of symmetry. A total of three hydride ligands (no structure implied) is indicated by the observation of a quartet in the ^{31}P NMR spectrum of **5** recorded with decoupling of the

(13) Fernández, M. J.; Rodriguez, M. J.; Oro, L. A.; Lahoz, F. J. *J. Chem. Soc., Dalton Trans.* **1989**, 2073−2079.

(14) Bovens, M.; Gerfin, T.; Gramlich, V.; Petter, W.; Venanzi, L. M.; Haward, M. T.; Jackson, S. A.; Eisenstein, O. *New. J. Chem.* **1992**, *16*, 337−345.

(15) Kang, J. W.; Moseley, K.; Maitlis, P. M. *J. Am. Chem. Soc.* **1969**, *91*, 5970−5977.

(16) May, S.; Reinsalu, P.; Powell, J. *Inorg. Chem.* **1980**, *19*, 1582−1589.

(17) Oldham, W. J., Jr.; Heinekey, D. M. Unpublished results.

(18) Paneque, M.; Poveda, M. L.; Toboada, S. *J. Am. Chem. Soc.* **1994**, *116*, 4519−4520.

Table 5. H−H Bond Lengths from T1(min) Data in the Limits of Slow and Fast Rotations

	H−H (Å)	
complex	slow rotation	fast rotation
$[TpIr(PMe_3)(H_2)H]^+$ (**5**)	1.11	0.88
$[TpIr(PPh_3)(H_2)H]^+$ (**6**)	1.12	0.89
$[TpRh(PPh_3)(H_2)H]^+$ (**8**)	0.92	0.73

organic protons. At all temperatures, only a single hydride resonance is observed in the ^1H NMR spectrum, which may result from a fluxional trihydride or a fluxional dihydrogen/hydride complex. These possibilites can be distinguished by a combination of $T_1(min)$ measurements and analysis of the effect of partial substitution of the hydride ligands with deuterium or tritium.

The minimum of the longitudinal relaxation time ($T_1(min)$) of the dihydrogen ligand has been shown to be a sensitive indicator of the H−H bond length.[4] The short $T_1(min)$ values observed for **5**−**8** are qualitatively consistent with the presence of a bound H_2 ligand in a dihydrogen/hydride structure. An accurate calculation of the H−H bond length requires that the mutual relaxation rate of the hydrogen atoms in the coordinated dihydrogen ligand (R_{d-d}) be known explicitly ($1/T_1$ = relaxation rate, R). The observed rate of dipolar relaxation for a dihydrogen ligand (R_{H_2}) is actually the sum of the mutual H−H dipolar relaxation (R_{d-d}) and the relaxation resulting from interactions with other dipoles in the molecule (R_o), thus $R_{H_2} = R_{d-d} + R_o$.[5] Additionally, in the case of fluxional polyhydride complexes suspected to contain a dihydrogen ligand, the observed $T_1(min)$ value is the population-weighted average of all the hydride sites. For the dihydrogen/hydride complexes under study in this work, the observed relaxation rate ($R_{obs} = 1/T_1$) is given by $R_{obs} = (2R_{H_2} + R_H)/3$ where R_{H_2} and R_H are the relaxation rates of the dihydrogen and hydride ligands. The relaxation rate of the terminal hydride ligand (R_H) can be estimated from the $T_1(min)$ value of the parent dihydrogen complexes such as **1**. Similarly, R_o can also be estimated from this measurement. Calculation of R_{d-d} for the dihydrogen ligand of **5** is shown as follows:

$$R_{obs}(\mathbf{5}) = (R_H + 2R_{H_2})/3 = (R_H + 2(R_{d-d} + R_o))/3$$

if R_H and $R_o \approx R_{obs}(\mathbf{1})$, then

$$R_{obs}(\mathbf{5}) = (2R_{d-d} + 3R_{obs}(\mathbf{1}))/3$$

and

$$R_{d-d} = 3(R_{obs}(\mathbf{5}) - R_{obs}(\mathbf{1}))/2 = 69 \text{ s}^{-1}$$

Similar calculations have been carried out for **6** and **8**. The H−H bond length can now be calculated in the limits of slow and fast hydrogen rotation by the method of Halpern and co-workers. We find that the H−H bond length of the dihydrogen ligand of **5** is bracketed by distances of 1.11 and 0.88 Å (Table 5). We can estimate the true H−H bond length after first considering the results obtained upon partial substitution of the hydride positions with deuterium or tritium.

Isotopic Perturbation of Equilibrium. We propose that the unusually large and temperature-dependent isotope shifts observed for the iridium dihydrogen/hydride complexes are a manifestation of isotopic perturbation of equilibria.[19] Generally only small (0−70 ppb) temperature-independent upfield isotope shifts are commonly observed upon partial substitution of

deuterium atoms in the hydride positions of dihydrogen and polyhydride complexes.[7,8,20−24] A few reports of downfield isotope shifts in both these classes of molecules have also appeared.[5,18,25−35] In some cases, the observed isotope shifts have been rationalized by invoking isotopic perturbation of equilibria;[10,27,34] however, a detailed study of this phenonenon has not been reported.

Two types of equilibrium situations may be perturbed upon substitution of the hydride positions of **5**−**7** with deuterium or tritium. The observed isotope shifts may result from perturbation of an equilibrium between a dihydrogen/hydride complex and a trihydride complex (eq 6).[27,36] A second possibility is

(6)

(7)
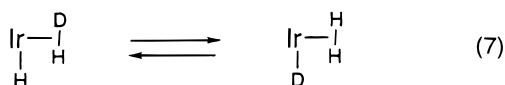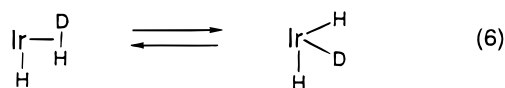
that, within a single dihydrogen/hydride ground state structure, the heavy hydrogen isotopes may concentrate in a particular site (eq 7). These two possibilities can be distinguished by comparing the isotope shifts upon partial deuteration using both ^1H and ^2H NMR spectroscopy. In our case, very broad lines were observed in the ^2H NMR spectra, so we instead incorporated tritium in the hydride positions and investigated this problem using ^1H and ^3H NMR spectroscopy. If the equilibrium in eq 6 is perturbed upon isotopic substitution, identical isotopomers will be observed at the same chemical shifts in the ^1H and ^3H NMR spectra, but the H_3 and T_3 isotopomers will not coincide.[37] If instead, an equilibrium between different sites in the same structure is perturbed (eq 7), then the H_3 and T_3 isotopomers will be observed at approximately the same

(19) Saunders, M.; Kates, M. R. *J. Am. Chem. Soc.* **1977**, *99*, 8070−8071.

(20) Hamilton, D. G.; Luo, X. L.; Crabtree, R. H. *Inorg. Chem.* **1989**, *28*, 3198−3203.

(21) Luo, X. L.; Crabtree, R. H. *J. Am. Chem. Soc.* **1990**, *112*, 4813−4821.

(22) Luo, X.; Michos, D.; Crabtree, R. H. *Organometallics* **1992**, *11*, 237−241.

(23) Baird, G. J.; Davies, S. G.; Moon, S. D.; Simpson, S. J.; Jones, R. H. *J. Chem. Soc., Dalton Trans.* **1985**, 1479−1486.

(24) Casey, C. P.; Tanke, R. S.; Hazin, P. N.; Kemnitz, C. R.; McMahon, R. J. *Inorg. Chem.* **1992**, *31*, 5474−5479.

(25) Heinekey, D. M.; Payne, N. G.; Sofield, C. D. *Organometallics* **1989**, *8*, 1824−1826.

(26) Antoniutti, S.; Albertin, G.; Amendola, P.; Bordignon, E. *J. Chem. Soc., Chem. Commun.* **1989**, 229−230.

(27) Earl, K. A.; Jia, G.; Maltby, P. A.; Morris, R. H. *J. Am. Chem. Soc.* **1991**, *113*, 3027−3039.

(28) Nanz, D.; von Philipsborn, W.; Bucher, U. E.; Venanzi, L. M. *Magn. Reson. Chem.* **1991**, *29*, S38−44.

(29) Michos, D.; Luo, X.; Crabtree, R. H. *Inorg. Chem.* **1992**, *31*, 4245−4250.

(30) Collman, J. P.; Wagenknecht, P. S.; Hutchison, J. E.; Lewis, N. S.; Lopez, M. A.; Guilard, R.; L'Her, M.; Bothner-By, A. A.; Mishra, P. K. *J. Am. Chem. Soc.* **1992**, *114*, 5654−5664.

(31) Miller, R. L.; Toreki, R.; LaPointe, R. E.; Wolczanski, P. T.; Van Duyne, G. D.; Roe, D. C. *J. Am. Chem. Soc.* **1993**, *115*, 5570−5588.

(32) Bianchini, C.; Linn, K.; Masi, D.; Peruzzini, M.; Polo, A.; Vacca, A.; Zanobini, F. *Inorg. Chem.* **1993**, *32*, 2366−2376.

(33) Heinekey, D. M.; Liegeois, A.; van Roon, M. *J. Am. Chem. Soc.* **1994**, *116*, 8388−8389.

(34) Albinati, A.; Bakhmutov, V. I.; Caulton, K. G.; Clot, E.; Eckert, J.; Eisenstein, O.; Gusev, D. G.; Grushin, V. V.; Hauger, B. E.; Klooster, W. T.; Koetzle, T. F.; McMullan, R. K.; O'Loughlin, T. J.; Pélissier, M.; Ricci, J. S.; Sigalas, M. P.; Vymenits, A. B. *J. Am. Chem. Soc.* **1993**, *115*, 7300−7312.

(35) Bullock, R. M.; Song, J.; Szalda, D. J. *Organometallics* **1996**, *15*, 2504−2516.

(36) Luo, X.; Crabtree, R. H. *J. Am. Chem. Soc.* **1990**, *112*, 6912−6918.

(37) An example of an equilibrium between two different structures has been characterized using this method by Hartwig and De Gala in the case of an equilibrium between a hydroborate and a boryl complex: Hartwig, J. F.; De Gala, S. R. *J. Am. Chem. Soc.* **1994**, *116*, 3661−3662.

chemical shift, but the isotope shifts observed in the ^{1}H NMR spectrum will be in the direction opposite to that observed in the ^{3}H NMR spectrum.[38] The spectra shown in Figure 4 and the data tabulated in Table 3 confirm that the isotope effect results from a nonstatistical site preference for deuterium (or tritium) in a single dihydrogen/hydride structure. That is, the equilibrium which is perturbed upon isotopic substitution is that described by eq 7. An important assumption which we make in the quantitative analysis outlined below is to ignore contributions from intrinsic isotope effects. We assume, for example, that the isotope shift in the ^{1}H NMR spectrum resulting from partial deuteration arises entirely from isotopic perturbation effects, rather than intrinsic isotope effects.

In principle, the observed chemical shifts and the J_{H-D} coupling data can be analyzed quantitatively to calculate the limiting chemical shifts of the dihydrogen ligand (δ_{H_2}) and the terminal hydride ligand (δ_H), $^1J_{H-D}$ for the dihydrogen ligand, and the energy difference between deuterium substitution of the dihydrogen site versus the hydride site. This method is based on the procedure used by Calvert and Shapley[39] in the study of fluxional agostic methyl groups. The general approach is to relate the dynamically averaged observables in the ^{1}H NMR spectrum (hydride chemical shifts and coupling constants) to the limiting values from which they originate.

The hydride chemical shift of the H_3 isotopomer (δ_{H_3}) is simply the statistical average of the dihydrogen site and the hydride site, thus $\delta_{H_3} = (2\delta_{H_2} + \delta_H)/3$. However, upon substitution of one deuterium atom in the hydride positions an equilibrium between three different species is obtained (eq 8).

$$(8)$$

$$(9)$$
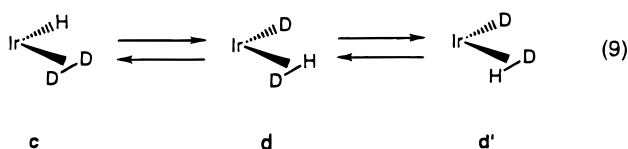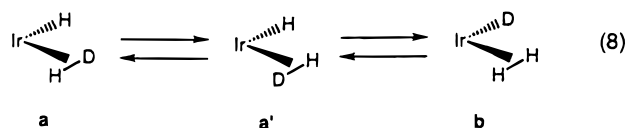
A similar equilibrium mixture is obtained if two deuterium atoms are incorporated in the hydride positions (eq 9). In this analysis we assume that there is no preference between **a** and **a′**. That is, **a** and **a′** are assumed to be degenerate. We also assume that the chemical shift of the *exo* hydrogen atom in **a** is the same as the *endo* hydrogen atom in **a′**. The observed chemical shift of the H_2D isotopomer is given by eq 10, where

$$\delta_{(H_2D)} = a\left(\frac{\delta_{H_2} + \delta_H}{2}\right) + a'\left(\frac{\delta_{H_2} + \delta_H}{2}\right) + b(\delta_{H_2}) \quad (10)$$

$$\delta_{(H_2D)} = \left(\frac{\delta_{H_2} + \delta_H + A_1\delta_{H_2}}{2 + A_1}\right) \quad (11)$$

a, a', and b are the mole fractions of each species. Within this definition, the sum of $a + a' + b = 1$. The Boltzmann factor A_1, defined as $e^{-\Delta E/RT}$, may be introduced to account for an energy difference between a (a') and b. A_1 is equal to $b/a = b/a'$. Thus a and a' can be combined and the mole fractions

(38) An example of an equilibrium between two different proton sites in the same structure, which has been characterized using both ^{1}H and ^{2}H NMR spectroscopy, is provided by Stone's investigation of [Fe_2(μ-CH_3)(μ-CO)(μ-dmpm)Cp_2]PF_6: Dawkins, G. M.; Green, M.; Orpen, A. G.; Stone, F. G. A. *J. Chem. Soc., Chem. Commun.* **1982**, 41−43.
(39) Calvert, R. B.; Shapley, J. R. *J. Am. Chem. Soc.* **1978**, *100*, 7726−7727.

can be rewritten in terms of the Boltzmann factor, A_1. For this problem, $a = a' = 1/(2 + A_1)$ and $b = A_1/(2 + A_1)$, leading to eq 11. In a similar fashion, the observed J_{H-D} coupling constant is given by eq 12. If the two-bond $^2J_{H-D}$ coupling between the

$$J_{(H_2D)} = a\left(\frac{^1J_{H-D} + {^2J_{H-D}}}{2}\right) + a'\left(\frac{^1J_{H-D} + {^2J_{H-D}}}{2}\right) + b(^2J_{H-D})$$

$$(12)$$

$$J_{(H_2D)} = \frac{^1J_{H-D}}{2 + A_1} \quad (13)$$

dihydrogen ligand and the terminal hydride ligand is assumed to be zero and the a and a' terms are combined, then the equation can be rewritten in terms of the Boltzmann factor, A_1, and simplified to give eq 13.

In a similar fashion, expressions can be derived which relate the chemical shift and observed J_{H-D} coupling of the HD_2 isotopomer, written in terms of a second Boltzmann factor, A_2. The observed ^{1}H resonance of the HD_2 isotopomer is given by eq 14, where c, d, and d' are the mole fractions of the species

$$\delta_{(HD_2)} = c(\delta_H) + d(\delta_{H_2}) + d'(\delta_{H_2}) \quad (14)$$

$$\delta_{(HD_2)} = \frac{2A_2\delta_{H_2} + \delta_H}{2A_2 + 1} \quad (15)$$

shown in eq 9. Analogous to the previous presentation, $c + d + d' = 1$ and the Boltzmann factor A_2 is equal to $d/c = d'/c$. Rewriting the mole fractions in terms of A_2, $c = 1/(2A_2 + 1)$ and $d = d' = A_2/(2A_2 + 1)$. Substituting these back into eq 14 leads to eq 15. The observed H−D coupling of the HD_2 isotopomer is given by eq 16. If the $^2J_{H-D}$ term is assumed to

$$J_{(HD_2)} = c(^2J_{H-D}) + d\left(\frac{^1J_{H-D} + {^2J_{H-D}}}{2}\right) + d'\left(\frac{^1J_{H-D} + {^2J_{H-D}}}{2}\right)$$

$$(16)$$

$$J_{(HD_2)} = \frac{^1J_{H-D}A_2}{2A_2 + 1} \quad (17)$$

be zero and the substitutions for the mole fractions are made, then eq 16 reduces to eq 17.

The results of this analysis (calculated using the data presented in Tables 2 and 3) for complexes **5**−**7** are presented in Table 6. In the case of **5**, the limiting spectroscopic parameters were also calculated at every temperature indicated in Figures 2 and 3. In this way, the standard deviation (or precision) in each calculated parameter for complex **5** was obtained: $\delta_{H_2} = -8.4 \pm 0.1$ ppm, $\delta_H = -14.4 \pm 0.3$ ppm, $^1J_{H-D} = 24.6 \pm 0.3$ Hz, $\Delta E_1 = -130 \pm 12$ cal/mol, and $\Delta E_2 = -107 \pm 12$ cal/mol. However, comparison of the results calculated from the ^{1}H and ^{3}H NMR data for complexes **6** and **7** indicates that systematic error introduces larger uncertainties in the calculated parameters than the precision of the measurement would suggest. The error in the calculated chemical shifts (estimated from the standard deviation of the two measurements) is approximately ±1 ppm. The error in the calculated energy differences is ±25%, and that in the calculated H−T coupling constants is ±4 Hz. Despite these uncertainties, the analysis does confirm that the heavy hydrogen isotope concentrates in the terminal hydride position. Thus, in relation to eqs 8 and 9, we conclude that the equilibria lie to the right. Because the chemical shift of the dihydrogen ligand is downfield of the hydride signal, this leads to the

Table 6. Calculated Parameters from Isotopic Perturbation Analysis of ^{1}H and ^{3}H NMR Spectra of **5**–**7** Acquired at 240 K

	5[a]	**5** (^{3}H)[b]	**6** (^{1}H)[c]	**6** (^{3}H)[b]	**7**[a]	**7** (^{1}H)[c]	**7** (^{3}H)[b]
δ_{H_2} (ppm)	−8.3	−8.3	−7.2	−8.0	−9.1	−8.7	−9.2
δ_H (ppm)	−14.6	−14.4	−14.6	−13.2	−15.0	−15.9	−14.8
$^1J_{H-D}$ (Hz)	24.7				24.8		
$^1J_{H-T}$ (Hz)		177	176	180		178	183
ΔE_1 (cal/mol)	−125[d]	−136[f]	−143[f]	−177[f]	−153[d]	−174[f]	−203[f]
ΔE_2 (cal/mol)	−103[e]	−110[g]	−143[g]	−99[g]	−118[e]	−171[g]	−132[g]

[a] ^{1}H NMR analysis of a partially deuterated sample. [b] ^{3}H NMR analysis of a partially tritiated sample. [c] ^{1}H NMR analysis of a partially tritiated sample. [d] Energy difference between Tp(L)Ir(HD)H and Tp(L)Ir(H$_2$)D (see eq 5). [e] Energy difference between Tp(L)Ir(D$_2$)H and Tp(L)Ir(HD)D (eq 6). [f] Energy difference between Tp(L)Ir(HT)H and Tp(L)Ir(H$_2$)T. [g] Energy difference between Tp(L)Ir(T$_2$)H and Tp(L)Ir(HT)T.

significant downfield shift in the ^{1}H NMR spectrum and the corresponding upfield shift in the ^{3}H NMR spectrum.

Structural Considerations. The above analysis establishes that a dihydrogen/hydride structure is adopted by complexes **5**–**8**. In contrast, the Cp (or Cp*) analogs such as [CpIr(PR$_3$)-H$_3$]$^+$ are trihydride complexes, with appropriately long T_1(min) values of *ca.* 300 ms.[7] Protonation of CpRh(PiPr$_3$)H$_2$ with HPF$_6$ is reported to yield a hydride-bridged dimer, [{CpRh(PiPr$_3$)}$_2$-(μ-H$_3$)]PF$_6$, and H$_2$.[39] Mononuclear rhodium analogs of [CpIr-(PR$_3$)H$_3$]$^+$ are not known. A similar change in structure from trihydride to dihydrogen/hydride upon substitution of Tp for Cp ligands has been reported by Chaudret and co-workers in related ruthenium complexes.[41,42] The neutral CpRu(PR$_3$)H$_3$ complexes are characterized as classical trihydride complexes;[43] however, substitution of the Cp ligand for Tp^{Me_2} results in stable complexes of the form Tp^{Me_2}Ru(L)(H$_2$)H. In this case, L can be a phosphine, nitrogen, or sulfur donor ligand.

In most cases, the Tp ligand is considered to be a more efficient donor than the Cp ligand.[9] This property would seem to favor a trihydride structure over the dihydrogen/hydride structure that is actually observed in this system. However, for the later transition metals such as iridium, the Tp ligand transfers less electron density to the metal center. This is reflected in the higher CO stretching frequency of TpIr(CO)H$_2$ (2020 cm^{-1}, CH$_2$Cl$_2$)[44] versus CpIr(CO)H$_2$ (2002 cm^{-1}, CH$_2$-Cl$_2$)[45] and also TpIr(CO)(C$_2$H$_4$) (2000 cm^{-1}, cyclohexane)[46] versus CpIr(CO)(C$_2$H$_4$) (1980 cm^{-1}, cyclohexane).[47] The difference in relative donor ability is probably a function of orbital overlap between iridium and the Cp or Tp ligands. The soft iridium center is expected to form stronger, more covalent bonds with the soft Cp ligand. The bonding between iridium and the hard pyrazolyl nitrogen donors is presumably more ionic in character. Steric factors will also favor complexes with a reduced coordination number for Tp (cone angle 184°) versus Cp (cone angle 136°) complexes.

Estimation of H−H Distances. As noted by Morris and co-workers, H−H bond distances inferred from T_1(min) data depend upon assumptions about the relative rate of dihydrogen rotation.[6] In the case of iridium complexes **5** and **6**, the observed T_1(min) values of 21–22 ms are consistent with an H−H distance of 0.88 Å (fast rotation) or 1.11 Å (slow rotation). Further insight can be obtained by making use of the roughly

linear inverse correlation between $^1J_{H-D}$ and the H−H bond length (determined by neutron diffraction or solid state NMR methods) as reported by Heinekey and Luther.[48] A similar analysis has been used to infer the relatively slow rotational motion of the dihydrogen ligand in [Cp*Ru(dppe)(H$_2$)]BF$_4$[49] and the dicationic complex [Os(bpy)(PPh$_3$)$_2$(CO)(H$_2$)](OTf)$_2$.[48] For the iridium complexes reported here, the H−D coupling in the bound dihydrogen ligand is *ca.* 25 Hz, which is consistent with an H−H distance of *ca.* 1 Å. These complexes may belong to the currently limited group of dihydrogen complexes such as [Os(H$_2$)(dppe)$_2$X]$^+$ (X = Cl, Br),[50] in which dihydrogen rotational motion is comparable to the rate of molecular tumbling.

In the case of the rhodium complex **8**, the H−H bond length is calculated to be between 0.92 Å (slow rotation) and 0.73 Å (fast rotation). Since the H−H bond length of free hydrogen is 0.74 Å, the value calculated by assuming fast rotation is probably not correct. Unfortunately, the rhodium complex gave only a broad hydride resonance upon partial deuteration of the hydride positions, so a J_{H-D} value is not available. Assuming that hydrogen rotation is relatively slow in complex **8**, as found for the iridium analogs, the longer H−H distance of *ca.* 0.92 Å results. Although a definitive value for the H−H distance in complex **8** cannot be obtained, it is clear that the H−H distance is significantly longer in the iridium complexes than for the corresponding rhodium complex.

Hydride Dynamics. Although a static low-temperature-limiting ^{1}H NMR spectrum was not obtained for complexes **5**–**8**, partial deuteration (tritiation) and the observation of IPR as detailed above allow the limiting chemical shifts δ_{H_2} and δ_H to be estimated. From these data and the observation of a single hydride resonance for **5** at 127 K, the activation energy for exchange between the dihydrogen ligand and the hydride ligand can be calculated as $\Delta G^{\ddagger} \leq 5$ kcal/mol. It should be noted that these observations were made on a sample of complex **5** which was heavily deuterated in the hydride positions. This rules out the possibility that exchange coupling could contribute to the observed spectrum as has been noted for other dynamic polyhydrides.[51]

While our data offer no mechanistic insight, it is instructive to consider possible mechanisms for the rapid exchange of all three hydride nuclei. Two distinct dynamic processes are required. Rotation of the dihydrogen ligand around the M−H$_2$ bond axis must be rapid on the chemical shift time scale. This is quite reasonable, since reported barriers to hydrogen rotation are very low, except in d^2 systems.[52,53] A second process

(40) Werner, H.; Wolf, J.; Höhn, A. *J. Organomet. Chem.* **1985**, *287*, 395−407.

(41) Moreno, B.; Sabo-Etienne, S.; Chaudret, B.; Rodriguez-Fernandez, A.; Jalon, F.; Trofimenko, S. *J. Am. Chem. Soc.* **1994**, *116*, 2635−2636.

(42) Moreno, B.; Sabo-Etienne, S.; Chaudret, B.; Rodriguez, A.; Jalon, F.; Trofimenko, S. *J. Am. Chem. Soc.* **1995**, *117*, 7441−7451.

(43) Arliguie, T.; Border, C.; Chaudret, B. *Organometallics* **1989**, *8*, 1308.

(44) Fernandez, M. J.; Rodriguez, M. J.; Oro, L. A. *J. Organomet. Chem.* **1992**, *438*, 337−342.

(45) Shapley, J. R.; Adair, P. C.; Lawson, J. R.; Pierpont, C. G. *Inorg. Chem.* **1982**, *21*, 1702−1704.

(46) Ciriano, M. A.; Fernández, M. J.; Modrego, J.; Rodríguez, M. J.; Oro, L. A. *J. Organomet. Chem.* **1993**, *443*, 249−252.

(47) Szajek, L. P.; Lawson, R. J.; Shapley, J. R. *Organometallics* **1991**, *10*, 357−361.

(48) Heinekey, D. M.; Luther, T. A. *Inorg. Chem.* **1996**, *35*, 4396−4399.

(49) Klooster, W. T.; Koetzle, T. F.; Jia, G.; Fong, T. P.; Morris, R. H.; Albinati, A. *J. Am. Chem. Soc.* **1994**, *116*, 7677−7681.

(50) Maltby, P. A.; Schlaf, M.; Steinbeck, M.; Lough, A. J.; Morris, R. H.; Klooster, W. T.; Koetzle, T. F.; Srivastava, R. C. *J. Am. Chem. Soc.* **1996**, *118*, 5396−5407.

(51) Heinekey, D. M.; Payne, N. G.; Sofield, C. D. *Organometallics* **1990**, *9*, 2643−2645.

(52) Jalón, F. A.; Otero, A.; Manzano, B. R.; Villaseñor, E.; Chaudret, B. *J. Am. Chem. Soc.* **1995**, *117*, 10123−10124.

exchanges hydrogen nuclei between the dihydrogen and the hydride ligands. Since our complexes are positively charged, it seems reasonable to speculate that a proton transfer may be involved, although it has been reported that the hydride ligands of the closely related ruthenium complexes $Tp^{Me_2}Ru(PR_3)(H_2)H$ also exchange rapidly on the NMR time scale. In this case, heterolytic cleavage of the dihydrogen ligand is not facilitated by an overall positive charge.[42]

Comparison with Related Complexes. There are several examples of fluxional *cis*-dihydrogen/hydride complexes in the literature. Partial deuteration has been generally employed to establish the presence of the H_2 ligand, but large isotope effects such as those observed for **5–7** have not been previously reported. A modest upfield isotope shift has been reported by Field and co-workers in $[Fe\{P(CH_2CH_2CH_2PMe_2)_3\}(H_2)H]$-$BPh_4$.[54] In this iron complex, $J_{H-D}(H_2D) > J_{H-D}(HD_2)$ (10 and 9 Hz, respectively), consistent with a slight preference for deuterium to concentrate in the dihydrogen ligand, opposite to the preference observed in **5–7**. Distinct hydride resonances attributed to the H_3 and the H_2D isotopomers are observed upon partial deuteration of $[Os\{P(CH_2CH_2PPh_2)_3\}(H_2)H]BPh_4$.[32] The reported isotope shifts are consistent with a modest preference for deuterium to concentrate in the hydride ligand; however, the temperature dependence of the isotope shifts was not reported. The observed H–D couplings for this osmium complex are nearly identical to the H–D coupling constants for **5** and **7**, indicating that the dihydrogen ligand in each of these complexes is in a similar electronic environment.

Large and temperature-dependent isotope effects have been reported in partially deuterated $Tp^{Me_2}IrH_4$, along with substantial H–D coupling, which is suggestive of a dihydrogen/dihydride structure. However, this complex has quite long hydride relaxation times, which led Poveda and co-workers to suggest a tetrahydride structure.[18] The corresponding rhodium complex $Tp^{Me_2}Rh(H_2)H_2$ has been formulated as a dihydrogen/dihydride species on the basis of the observation of H–D coupling and short T_1 values for the hydride ligands.[28] The apparent structural difference between these two complexes rests primarily on T_1 data. Further structural information on these interesting complexes would be very desirable.

Conclusion

Protonation of $TpM(PR_3)H_2$ (M = Rh, Ir) complexes affords highly dynamic dihydrogen/hydride complexes. In the case of the iridium complexes, partial substitution of the hydride positions with deuterium or tritium results in large temperature-dependent isotope shifts, which result from a preference for the heavy isotope to occupy the hydride site. Analysis of these data gives the limiting chemical shifts of the dihydrogen and hydride ligands as well as the coupling constant $^1J_{H-D}$ of the dihydrogen ligand (*ca.* 25 Hz). These observations, combined with short $T_1(min)$ values of *ca.* 22 ms for the Ir complexes, are consistent with an H–H bond length of *ca.* 1 Å. For the Rh complex, the $T_1(min)$ value of 7 ms is consistent with the presence of a bound dihydrogen ligand, but H–D coupling was not resolvable. The T_1 data for the Rh complex give an H–H distance of 0.73–0.92 Å, depending on the rate of dihydrogen rotation.

Experimental Section

General Methods. All manipulations were conducted under a dry argon or nitrogen atmosphere using standard Schlenk and drybox techniques. Solvents were purified by distillation from Na–K–

benzophenone (except CH_2Cl_2 from P_2O_5) under a nitrogen atmosphere. Deuterated NMR solvents (purchased from Cambridge Isotope Laboratories) were degassed and were stored over CaH_2 (CD_2Cl_2) or Na–K–benzophenone (C_6D_6, toluene-d_8, THF-d_8). Hydrogen (99.999%) and ethylene (99.7%) were purchased from Airco. Potassium hydrotris-(1-pyrazolyl)borate (KTp) was prepared by the procedure of Trofimenko.[55] $RhCl_3 \cdot 3H_2O$ was purchased from Pressure Chemicals. $(NH_4)_2IrCl_6$ was recovered from laboratory iridium residues by following published procedures.[56] Unless stated otherwise, all other reagents were obtained from Aldrich and used as received.

Variable-temperature NMR measurements were performed using the Bruker B-VT1000 temperature control module with a copper–constantan thermocouple. Temperature calibration was obtained by measurement of the chemical shift difference between the –CH_3 and –OH peaks of a standard methanol sample using the method of Van Geet.[57] Tritium NMR spectra were obtained on a Bruker WM-500 spectrometer at 533 MHz with a Cryomagnetics tritium probe and externally referenced to $(CHDTCO_2)^-$.[58] The procedures employed to safely store and manipulate tritium gas have been described previously.[8]

Infrared spectra were recorded as Nujol mulls between NaCl plates on a Perkin-Elmer model 1600 Fourier transform spectrophotometer (2.0 cm^{-1} resolution). Elemental analyses were performed by Canadian Microanalytical Services, Ltd., Vancouver, BC, Canada.

$[(C_5Me_5)Ir(PMe_3)H_3]SO_3CF_3$. To a 300 mL glass bomb fitted with a Kontes valve were added $(C_5Me_5)Ir(PMe_3)Cl_2$[59] (2.01 g, 4.24 mmol) and $AgSO_3CF_3$ (2.37 g, 9.2 mmol). CH_2Cl_2 (50 mL) was vacuum-transferred into the flask and the head space backfilled with H_2 (1000 Torr). The flask was covered with aluminum foil, and the mixture was allowed to stir overnight to yield a pale orange solution containing a white precipitate (AgCl), which was filtered off. The volume of the filtrate was reduced under vacuum. Layering with Et_2O gave colorless crystals upon standing at –30 °C for 3 days. These were washed with Et_2O (3 × 5 mL) and dried under vacuum. Yield: 2.06 g (88%). The ^1H NMR spectrum of the product matches that previously reported.[60]

$[(C_5Me_5)Ir(PPh_3)H_3]BF_4$. This complex was prepared from $(C_5-Me_5)Ir(PPh_3)Cl_2$[15] as above but using $AgBF_4$. Yield: 60%. The product was characterized by ^1H NMR spectroscopy.[11]

$TpIr(PMe_3)H_2$ (1). A solution of $[(C_5Me_5)Ir(PMe_3)H_3]SO_3CF_3$ (146 mg, 0.263 mmol) in CH_3CN (15 mL) was stirred under Ar at room temperature for 2 days. NaTp (66 mg, 0.280 mmol) was added. After the mixture was stirred for an additional 2 days, the volatiles were removed under vacuum and the resulting residue was taken up in a minimum of toluene. Complex **1** was isolated by chromatography on alumina, eluting with toluene. The toluene was removed by rotary evaporation and the residue crystallized by adding wet MeOH. The resulting white powder was dried under vacuum to yield 70 mg (55%) of analytically pure product. ^1H NMR, δ (CD_2Cl_2): 7.70, 7.63 (d, 2 H each, 3,5-pz$_{eq}$); 7.67, 7.59 (m, 1 H each, 3,5-pz$_{ax}$); 6.18 (t, 2 H, 4-pz$_{eq}$); 6.08 (m, 1 H, 4-pz$_{ax}$); 1.63 (d, J_{P-H} = 10.0 Hz, 9 H, PMe$_3$); –21.3 (d, J_{P-H} = 25.0 Hz, 2 H, Ir–H). $^{13}C\{^1H\}$ NMR, δ (CD_2Cl_2): 146.2, 134.0 (s, 1 C, 3,5-pz$_{ax}$); 144.0, 138.8 (s, 2 C, 3,5-pz$_{eq}$); 105.8 (s, 1 C, 4-pz$_{ax}$); 105.6 (s, 2 C, 4-pz$_{eq}$); 21.7 (d, J_{P-C} = 39.4 Hz). $^{31}P\{Me^1H\}$ NMR, δ (CD_2Cl_2): –45.6 (t, J_{P-H} = 25 Hz). ^1H NMR (C_6D_6): 7.93, 7.34 (br s and m, respectively, 1 H each, 3,5-pz$_{ax}$); 7.57, 7.53 (d, 2 H each, 3,5-pz$_{eq}$); 5.94 (t, 2 H, 4-pz$_{eq}$); 5.68 (m, 1 H, 4-pz$_{ax}$); 1.32 (d, J_{P-H} = 9.9 Hz, PMe$_3$); –20.56 (d, J_{P-H} = 25.5 Hz, 2 H, Ir–H). $^{13}C\{^1H\}$, δ NMR, δ (C_6D_6): 146.4, 133.3 (s, 1 C each, 3,5-pz$_{ax}$); 144.1, 134.4 (s, 2 C, 3,5-pz$_{eq}$); 105.7 (s, 1 C, 4-pz$_{ax}$); 105.4 (s, 2 C, 4-pz$_{eq}$); 21.5 (d, J_{P-C} = 38.8 Hz, PMe$_3$). $^{31}P\{Me^1H\}$ NMR, δ (C_6D_6): –46.55 (t, J_{P-H} = 24.3 Hz). IR cm^{-1}: 2482 (ν_{B-H}); 2143 (ν_{Ir-H}). MS: *m/z* 484 (M$^+$). Anal. Calcd for $C_{12}H_{21}BIrN_6P$: C, 29.83; H, 4.38; N, 17.39. Found: C, 29.51; H, 4.83; N, 17.26.

$TpIr(PPh_3)H_2$ (2). This complex was prepared as above, starting from $[(C_5Me_5)Ir(PPh_3)H_3]BF_4$. Yield: 60%. ^1H NMR (C_6D_6): 8.04,

(53) Sabo-Etienne, S.; Chaudret, B.; el Makarim, H. A.; Barthelat, J.; Daudey, J.; Ulrich, S.; Limbach, H.; Moïse, C. *J. Am. Chem. Soc.* **1995**, *117*, 11602–11603.

(54) Bampos, N.; Field, L. D. *Inorg. Chem.* **1990**, *29*, 587–588.

(55) Trofimenko, S. *Inorg. Synth.* **1979**, *12*, 99.

(56) Kauffman, G. B.; Myers, R. D. *Inorg. Synth.* **1978**, *18*, 131–133.

(57) Gordon, A. J.; Ford, R. A. *The Chemist's Companion*; Wiley: New York, 1972; p 303.

(58) Evans, E. A.; Warrell, D. C.; Elvidge, J. A.; Jones, J. R. *Handbook of Tritium NMR Spectroscopy and Applications*; Wiley: New York, 1985.

(59) Isobe, K.; Bailey, P. M.; Maitlis, P. M. *J. Chem. Soc., Dalton Trans.* **1981**, 2003–2008.

(60) Gilbert, T. M.; Bergman, R. G. *J. Am. Chem. Soc.* **1985**, *107*, 3502–3507.

7.35 (br s and m, respectively, 1 H each, 3,5-pz$_{ax}$); 7.66−7.59 (m, 6 H, PPh$_3$); 7.49, 6.85 (d, 2 H each, 3,5-pz$_{eq}$); 6.99−6.95 (m, 9 H, PPh$_3$); 5.75 (m, 1 H, 4-pz$_{ax}$); 5.67 (t, 2 H, 4-pz$_{eq}$); −19.70 (d, 2 H, J_{P-H} = 23.1 Hz, Ir−*H*). ^{31}P{aromatic ^{1}H} NMR, δ (C$_6$D$_6$): 18.8 (t, J_{P-H} = 22.3 Hz). ^{1}H NMR (CD$_2$Cl$_2$): 7.83, 7.63 (br s and m, respectively, 1 H each, 3,5-pz$_{ax}$); 7.66, 6.61 (d, 2 H each, 3,5-pz$_{eq}$); 7.39−7.24 (m, 15 H, PPh$_3$); 6.13 (m, 1 H, 4-pz$_{ax}$); 5.86 (t, 2 H, 4-pz$_{eq}$); −20.47 (d, J_{P-H} = 22.1 Hz, 2 H, Ir−*H*). ^{13}C{^{1}H} NMR, δ (CD$_2$Cl$_2$): 146.4, 134.8 (s, 1 C, 3,5-pz$_{ax}$); 143.3, 134.7 (s, 2 C, 3,5-pz$_{eq}$); 135.3 (d, J_{P-C} = 56 Hz, *i*-C$_6$H$_5$); 134.2, 128.2 (d, J_{P-C} = 10 Hz, *o*- and *m*-C$_6$H$_5$); 130.1 (s, *p*-C$_6$H$_5$); 106.0 (s, 1 C, 4-pz$_{ax}$); 105.2 (s, 2 C, 4-pz$_{eq}$). ^{31}P{aromatic ^{1}H} NMR, δ (CD$_2$Cl$_2$): 16.9 (t, J_{P-H} = 22.0 Hz). IR, cm^{-1}: 2481 (ν_{B-H}); 2179, 2139 (ν_{Ir-H}). Anal. Calcd for C$_{27}$H$_{27}$BIrN$_6$P: C, 48.44; H, 4.07; N, 12.55. Found: C, 48.20; H, 4.01; N, 12.24.

Tp^{Me_2}Ir(PMe$_3$)H$_2$ (3). This complex was prepared on a 1.5 mmol scale by a procedure identical to that described for the Tp analog. Yield: 74%. ^{1}H NMR, δ (CD$_2$Cl$_2$): 5.84 (s, 2 H, 4-pz$_{eq}$); 5.70 (s, 1 H, 4-pz$_{ax}$); 2.41, 2.26 (s, 6 H each, 3,5-Me$_2$pz$_{eq}$); 2.26, 2.09 (s, 3 H each, 3,5-Me$_2$pz$_{ax}$); 1.63 (d, J_{P-H} = 9.6 Hz, 9 H, PMe$_3$); −22.11 (d, J_{P-H} = 26.7 Hz, 2 H, Ir−*H*). ^{13}C{^{1}H} NMR, δ (CD$_2$Cl$_2$): 150.8, 144.7 (3,5-pz$_{eq}$); 150.0, 143.5 (3,5-pz$_{ax}$); 106.0 (4-pz$_{eq}$); 104.7 (4-pz$_{ax}$); 24.2 (d, J_{P-C} = 38.2 Hz, PMe$_3$); 17.35, 13.0 (3,5-Me$_2$pz$_{eq}$); 17.75, 12.7 (3,5-Me$_2$pz$_{ax}$). ^{31}P{^{1}H} NMR, δ (CD$_2$Cl$_2$): −53.0 (s). ^{1}H NMR, δ (C$_6$D$_6$): 5.76 (s, 2 H, 4-pz$_{eq}$); 5.47 (s, 1 H 4-pz$_{ax}$); 2.41, 2.10 (s, 3 H each, 3,5-Me$_2$pz$_{ax}$); 2.30, 2.27 (s, 6 H, 3,5-Me$_2$pz$_{eq}$); 1.41 (d, J_{P-H} = 9.6 Hz, 9 H, PMe$_3$); −21.21 (d, J_{P-H} = 26.1 Hz, 2 H, Ir−*H*). ^{13}C{^{1}H} NMR, δ (C$_6$D$_6$): 150.5, 144.1 (3,5-pz$_{eq}$); 149.8, 142.4 (3,5-pz$_{ax}$); 106.0 (4-pz$_{eq}$); 104.9 (4-pz$_{ax}$); 23.6 (d, J_{P-C} = 37.3 Hz, PMe$_3$); 17.5, 12.9 (3,5-Me$_2$pz$_{eq}$); 17.6, 12.6 (3,5-Me$_2$pz$_{ax}$). ^{31}P{Me ^{1}H} NMR, δ (C$_6$D$_6$): −52.0 (t, J_{P-H} = 24.7 Hz). IR, cm^{-1}: 2511 (ν_{B-H}); 2138 (ν_{Ir-H}). Anal. Calcd for C$_{18}$H$_{33}$BIrN$_6$P: C, 38.10; H, 5.86; N, 14.81. Found: C, 38.67; H, 5.94; N, 14.55.

[TpIr(PMe$_3$)(H$_2$)H]BF$_4$ (5). To a 50 mL Schlenk flask containing a solution of **1** (24 mg, 0.050 mmol) in Et$_2$O (5 mL) at −78 °C was added HBF$_4$·Et$_2$O (85%, 10 mL, 0.07 mmol) dropwise. The mixture was allowed to gradually warm to room temperature as fine white microcrystals precipitated from solution. The product was filtered off, washed with Et$_2$O (2 mL), and dried under vacuum. Yield: 87%. ^{1}H NMR, δ (CD$_2$Cl$_2$): 7.87, 7.85 (d, 2 H each, 3,5-pz$_{eq}$); 7.69, 7.67 (br s, 1 H each, 3,5-pz$_{ax}$); 6.43 (t, 2 H, 4-pz$_{eq}$); 6.21 (m, 1 H, 4-pz$_{ax}$); 1.78 (d, J_{P-H} = 11 Hz, 9 H, PMe$_3$); −10.40 (d, J_{P-H} = 11 Hz, 3 H, Ir−*H*). ^{13}C{^{1}H} NMR, δ (CD$_2$Cl$_2$): 146.1, 135.8 (3,5-pz$_{ax}$); 144.9, 136.8 (3,5-pz$_{eq}$); 107.8 (4-pz$_{eq}$); 107.3 (4-pz$_{ax}$); 17.9 (d, J_{P-C} = 42.9 Hz, PMe$_3$). ^{31}P{Me ^{1}H} NMR (CD$_2$Cl$_2$): −42.7 (q, J_{P-H} = 9.8 Hz). ^{1}H NMR, δ (CDCl$_2$F): 7.87, 7.79 (d, 2 H each, 3,5-pz$_{eq}$); 7.68, 7.59 (br s, 1 H each, 3,5-pz$_{ax}$); 6.40 (t, 2 H, 4-pz$_{eq}$); 6.13 (m, 1 H, 4-pz$_{ax}$); 1.76 (d, J_{P-H} = 11.6 Hz, 9 H, PMe$_3$); −10.42 (d, J_{P-H} = 10.5 Hz, 3 H, Ir−*H*). IR, cm^{-1}: 2499 (ν_{B-H}); 2199 (ν_{Ir-H}). Anal. Calcd for C$_{12}$H$_{22}$B$_2$F$_4$IrPN$_6$: C, 25.24; H, 3.88; N, 14.72. Found: C, 25.45; H, 4.03; N, 14.40.

[TpIr(PPh$_3$)(H$_2$)H]BF$_4$ (6). Methylene chloride was added dropwise to a suspension of TpIr(PPh$_3$)H$_2$ in Et$_2$O until a homogeneous solution was obtained. To this solution was added 1 equiv of HBF$_4$·Et$_2$O, and the mixture was then reduced in volume under vacuum and stored at −30 °C overnight to afford a colorless powder, which was filtered off, washed with Et$_2$O, and dried under vacuum. This material did not give a satisfactory elemental analysis. A color change from white to pale pink was observed when this complex was exposed to vacuum. Decomposition following loss of H$_2$ may explain the unsatisfactory analytical data. ^{1}H NMR, δ (CD$_2$Cl$_2$): 7.83, 6.79 (d, 2 H each, 3,5-pz$_{eq}$); 7.76, 7.70 (m, 1 H each, 3,5-pz$_{ax}$); 7.58 (m, 3 H, *p*-C$_6$H$_6$); 7.44, 7.16 (m, 6 H each, *o*- and *m*-C$_6$H$_6$); 6.25 (m, 1 H, 4-pz$_{ax}$); 6.09 (t, 2 H,

4-pz$_{eq}$); −9.77 (br, 3 H, Ir−*H*). ^{31}P{^{1}H} NMR, δ (CD$_2$Cl$_2$): 1.1 (s). IR, cm^{-1}: 2502 (ν_{B-H}); 2197 (ν_{Ir-H}). Anal. Calcd for C$_{27}$H$_{28}$B$_2$F$_4$IrN$_6$P: C, 42.83; H, 3.73; N, 11.1. Found: C, 40.00; H, 4.25; N, 9.20.

[Tp^{Me_2}Ir(PMe$_3$)(H$_2$)H][B(3,5-(CF$_3$)$_2$C$_5$H$_3$)$_4$] (7). A typical sample was prepared by vacuum transfer of CD$_2$Cl$_2$ (0.4 mL) into an NMR tube containing Tp^{Me_2}Ir(PMe$_3$)H$_2$ (12.8 mg, 0.023 mmol) and [H(Et$_2$O)$_2$]-[B(3,5-(CF$_3$)$_2$C$_6$H$_3$)$_4$]^{61} (23 mg, 0.023 mmol). ^{1}H NMR, δ (CD$_2$Cl$_2$): 7.73 (br, 8 H, *o*-C$_6$H$_3$(CF$_3$)$_2$); 7.58 (s, 4 H, *p*-C$_6$H$_3$(CF$_3$)$_2$); 6.08 (s, 2 H, 4-pz$_{ax}$); 5.75 (s, 1 H, 4-pz$_{ax}$); 2.46, 2.35 (s, 6 H each, 3,5-pz$_{eq}$); 2.25, 2.06 (s, 3 H each, 3,5-pz$_{ax}$); 1.63 (d, J_{P-H} = 10.7 Hz, 9 H, PMe$_3$); −11.0 (vbr, 3 H, Ir−*H*). ^{31}P{^{1}H} NMR, δ (CD$_2$Cl$_2$): −49.2 (s).

[TpRh(PPh$_3$)(H$_2$)H][B(3,5-(CF$_3$)$_2$C$_5$H$_3$)$_4$] (8). A typical sample was prepared by vacuum transfer of CD$_2$Cl$_2$ into an NMR tube containing TpRh(PPh$_3$)H$_2$ (2.6 mg, 0.0045 mmol) and [H(Et$_2$O)$_2$][B(3,5-(CF$_3$)$_2$-C$_6$H$_3$)$_4$] (5 mg, 0.0049 mmol). The sample was warmed to −78 °C and stored at this temperature until immediately before being transferred to a precooled NMR probe (< 250 K). ^{1}H NMR, δ (CD$_2$Cl$_2$): 7.80, 6.57 (d, 2 H each, 3,5-pz$_{eq}$); 7.72 (br, 8 H, *o*-C$_6$H$_3$(CF$_3$)$_2$); 7.57 (br, shoulder on *p*-C$_6$H$_3$(CF$_3$)$_2$ resonance); 7.54 (br, 3 H, *p*-C$_6$H$_3$(CF$_3$)$_2$); 7.41, 7.09 (m, 6 H each, *o*- and *m*-C$_6$H$_5$PPh$_2$); 6.22 (br m, 1 H, 4-pz$_{ax}$); 6.02 (t, 2 H, 4-pz$_{eq}$); −7.95 (br, 3 H, Rh−*H*).

X-ray Structure of [TpIr(PMe$_3$)(H$_2$)H]BF$_4$·CH$_2$Cl$_2$. Colorless crystals suitable for X-ray diffraction were obtained by diffusion of Et$_2$O into a solution of [TpIr(PMe$_3$)(H$_2$)H]BF$_4$ in CH$_2$Cl$_2$. Diffraction measurements were made on a crystal fragment of dimensions 0.3 × 0.3 × 0.35 mm in a nitrogen stream at 183 K on an Enraf-Nonius CAD4 diffractometer using graphite-monochromated Mo Kα radiation (λ = 0.710 73 Å). An orientation matrix was determined from 24 centered peaks in the range of 28° ≤ 2θ ≥ 34°. Monoclinic symmetry (space group *P*2$_1$/*n*) was indicated on the basis of systematic absences. The cell parameters are *a* = 10.560(2) Å, *b* = 13.500(3) Å, *c* = 15.880-(3) Å, β = 92.54(3)°, and *V* = 2261.6(11) Å^3 (*Z* = 4) with a calculated density of 1.918 g/cm^3. There were 3960 unique reflections collected, with 2θ ≤ 50°; of those reflections, 3196 with *I* ≥ 4σ(*I*) were adjudged observed. Reduction of the data was carried out with XCAD4, and further work was carried out using the Siemens version of SHELX.

The structure was solved by direct methods and agreed with the results of a Patterson function; location of the iridium atom reduced the *R* factor to 22%. The rest of the atoms were found from difference maps. The full refinement proceeded to a final *R* of 4.5% and an *R*$_w$ of 5.9%, with a GOF of 1.9. The weighting scheme required a correction factor of 0.0015. Tables of data collection, solution, and refinement details, crystal data, atomic coordinates, and anisotropic thermal parameters are included in the Supporting Information.

Supporting Information Available: An ORTEP drawing and tables giving a structure determination summary, positional parameters, thermal parameters, bond distances, and bond angles for [TpIr(PMe$_3$)(H$_2$)H]BF$_4$ (**5**) (9 pages). Ordering information and Internet access instructions are given on any current masthead page.

(61) Brookhart, M.; Grant, B.; Volpe, A. F., Jr. *Organometallics* **1992**, *11*, 3920−3922.